phys. stat. sol. (RRL) **2**, No. 3, 120–122 (2008) / **DOI** 10.1002/pssr.200802052

pss +++rapid research letters+++
www.pss-rapid.com

Structure, morphology, and growth dynamics of perfluoro-pentacene thin films

Stefan Kowarik[*,1], Alexander Gerlach[1], Alexander Hinderhofer[1], Silvia Milita[2], Francesco Borgatti[3], Federico Zontone[4], Toshiyasu Suzuki[5], Fabio Biscarini[3], and Frank Schreiber[1]

[1] IAP, Universität Tübingen, Auf der Morgenstelle 10, 72076 Tübingen, Germany
[2] CNR-IMM, Bologna, Via P. Gobetti 101, 40129 Bologna, Italy
[3] CNR-Istituto per lo Studio dei Materiali Nanostrutturati (ISMN), Bologna, Via P. Gobetti 101, 40129 Bologna, Italy
[4] ESRF, BP 220, 38043 Grenoble, France
[5] Institute for Molecular Science, Myodaiji, Okazaki 444-8787, Japan

Received 19 March 2008, accepted 2 April 2008
Published online 8 April 2008

PACS 61.05.cm, 61.66.Hq, 68.35.bm, 68.35.Ct, 68.55.am

[*] Corresponding author: e-mail stefan.kowarik@berkeley.edu

We report high structural order in thin films of the organic semiconductor perfluoro-pentacene (PFP), which is a candidate material for n-type applications, deposited by vacuum sublimation on oxidized silicon wafers. Bragg reflections up to high order in both specular and grazing incidence geometries and a mosaicity of less than 0.01° demonstrate the well defined structure. The thin film entirely consists of crystallites with a structure close to the bulk phase without any contamination with a second phase. Real-time X-ray measurements show that PFP grows in a Stranski–Krastanov growth mode with the first monolayer wetting the substrate before 3d-growth sets in during growth of the second monolayer. Implications for its use are discussed.

Successful demonstrations of organic electronic and optoelectronic devices have led to increasing interest in organic semiconducting materials, with pentacene (PEN) being the dominant material for p-type OFETs [1]. For organic molecular materials, tuning of e.g. energy levels is possible by exchanging functional groups in the molecular building block [2], and remarkable first results have been achieved with the PEN derivative perfluorinated pentacene ($C_{22}F_{14}$, PFP) [3]. Interesting optical properties have been found [4] and the electron transfer mechanisms from/to the substrate have been investigated for PFP [5]. High electron mobility is found in PFP [3] and it is structurally similar to and thus compatible with PEN [6] which makes it attractive for bipolar devices such as p–n junctions of PEN and PFP. High performance complementary circuits of PEN and PFP have already been demonstrated [3]. Further uses may involve 'seed-layers' of PFP to grow PEN, which will influence the injection barriers [5] and because of a similar lattice constant may lead to continuous growth at the PEN/PFP interface [3]. Still missing is the detailed understanding of the PFP thin film structure, the issue of polymorphism, and the growth mode of PFP, which are known to be crucial for device performance [7]. In this letter we report high structural order in thin films of the n-type semiconductor PFP on silicon-dioxide surfaces and determine their crystal structure, which we find to be close to the bulk unit cell. Further, we show in real-time experiments that PFP grows in a Stranski–Krastanov mode.

Real-time X-ray reflectivity, grazing-incidence X-ray diffraction, and noncontact atomic-force microscopy were performed to highlight different aspects of the structural order and the time evolution during growth. The silicon substrates with native oxide (thickness ~10 Å) were sonicated in acetone and isopropanol, and then rinsed with ultrapure water, followed by heating to 400 °C in vacuum. PFP layers were evaporated after thorough outgassing of the raw material under high vacuum conditions (base pressure $p = 1 \times 10^{-8}$ mbar) with a growth rate of 0.5 Å/min onto

substrates held at 10 °C, 30 °C, and 70 °C. X-ray measurements were performed in-situ in a portable vacuum chamber equipped with a beryllium window and evaporation cells, while atomic force measurements were performed ex-situ using a Veeco Dimension V AFM. The X-ray measurements were carried out at beamline ID10B at the ESRF in Grenoble, France, with a wavelength of 0.9291 Å.

Figure 1a shows a typical scan of the specular rod of a PFP thin film ($D_{PFP} = 210 \pm 10$ Å, 70 °C). For all samples also including films prepared at 30 °C substrate temperature, Bragg reflections associated with the PFP film at least up to the eighth order are visible from which an out-of-plane lattice constant of 15.7 Å is derived, i.e. PFP molecules have an upright orientation similar to PEN films. Roughness-damped interference fringes can be seen at low q_z in the range of 0–0.1 Å^{-1} ("Kiessig fringes"), the periodicity of which is associated with the total film thickness via $\Delta q_z = 2\pi/D_{tot}$, while fringes around the Bragg reflections ("Laue oscillations") are related to the coherently ordered film thickness via $\Delta q_z = 2\pi/D_{coh}$. Both Kiessig and Laue oscillations exhibit the same periodicity, showing that PFP films are coherently ordered throughout their entire thickness. A very small mosaicity of the crystalline PFP domains lower than 0.01° is obtained from a rocking scan on the first order Bragg reflection, which together with the large number of Bragg reflections is evidence of the high structural order in the PFP films.

For a more detailed investigation of the thin film crystal structure, we have used in-situ grazing incidence X-ray diffraction (GIXD) employing a point detector (see Fig. 1b) as well as a 2d-CCD camera. The positions of the thin film Bragg reflections correspond to a nearly orthorhombic lattice with unit cell dimensions of $a = 15.7$ Å, $b = 4.531$ Å, and $c = 11.40$ Å which are very close to the published bulk structure [3]. We therefore conclude that the PFP film structure is very similar to the bulk structure and importantly both at 70 °C and 30 °C substrate temperature we observe no phase coexistence between a thin film phase and a bulk phase in contrast to PEN under the corresponding conditions.

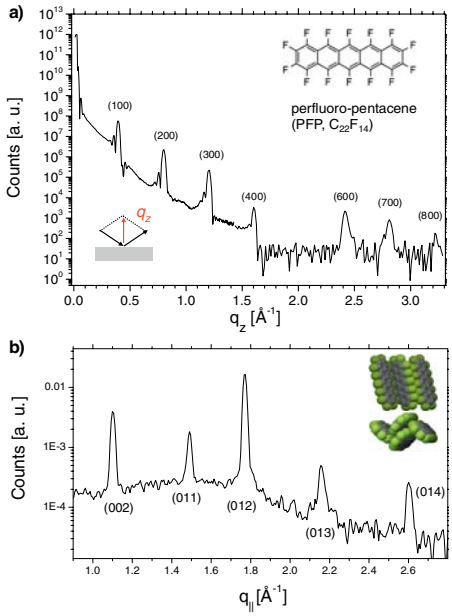

Figure 1 (online colour at: www.pss-rapid.com) a) Specular X-ray reflectivity of a 210 Å PFP film. Bragg reflections up to the eighth order can be seen, demonstrating high out-of-plane structural order. Inset: the PFP molecule. b) In-situ grazing incidence X-ray diffraction (GIXD) on a PFP thin film. Inset: molecular arrangement in the bulk structure which we find to be close to the film structure.

To investigate the morphology of PFP on silicon oxide we performed non-contact AFM measurements, as shown in Fig. 2. PFP forms elongated crystalline domains which are several microns in length, as has been described before [6]. This value is much larger than the coherently ordered size of PFP islands which is extracted from the width of the GIXD reflections in Fig. 1b to be ≥38 nm, indicating that each island seen with the AFM is composed of several smaller grains. Also from the presence of a large number of twinned crystals in Fig. 2a a high density of dislocations within the film can be inferred. The length of the grains diminishes for growth at 30 °C [4], but the overall morphology is very similar at both temperatures. In the AFM image, molecular terraces with monomolecular step height of ~15 Å are observed as shown in Fig. 2b and c, again confirming that molecules in the film have an upright orientation.

The steep pyramidal structures as observed in the AFM images show that PFP does not grow in a smooth layer-by-layer fashion but exhibits pronounced 3d-growth, similar to PEN where 3d-growth sets in after deposition of four monolayers [8]. For a quantitative understanding of the PFP growth behavior we measured anti-Bragg oscillations at $q_z = (1/2)\, q_{Bragg}$ and we also followed the evolution of the X-ray reflectivity in a wide q_z-range in real-time (Fig. 3a).

At the anti-Bragg point an oscillation with a period of two monolayers is expected as consecutive layers interfere destructively [8]. The PFP anti-Bragg oscillation exhibits a

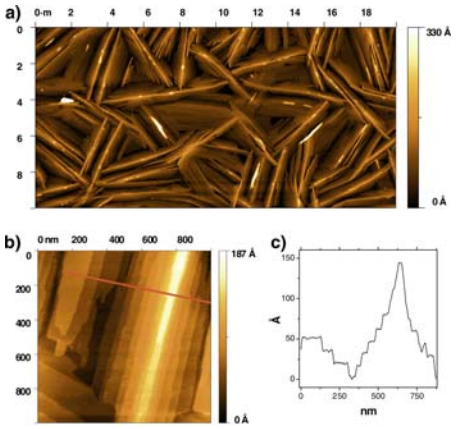

Figure 2 (online colour at: www.pss-rapid.com) a) AFM image of a PFP film grown at 70 °C substrate temperature on silicon oxide (thickness 220 ± 15 Å). b) Magnified image showing monomolecular terraces. c) Height profile along the line indicated in (b).

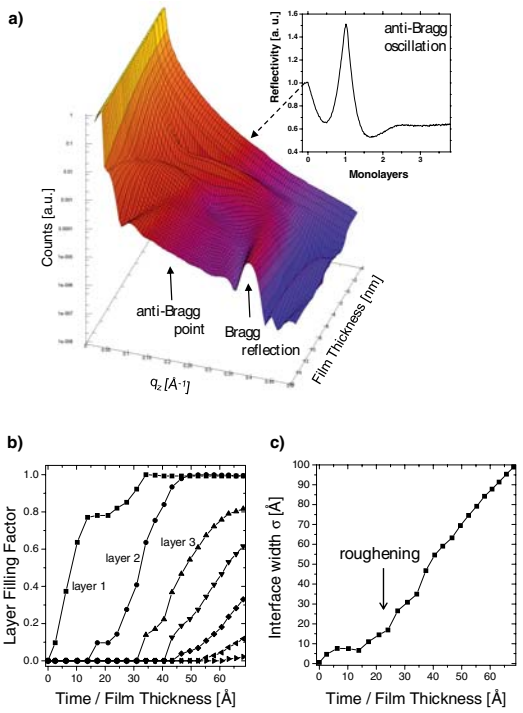

Figure 3 (online colour at: www.pss-rapid.com) a) Real-time evolution of the reflectivity during PFP growth. The damping of the anti-Bragg oscillation (inset) demonstrates the change from layer-by-layer growth to 3d-growth. The quantitative analysis of the 3d-dataset in (a) yields the time evolution of the filling factors of individual molecular layers (b) as well as the roughness evolution during growth (c).

sharp cusp when the coverage reaches one monolayer, due to the fact that there is a discrete shift from adding material to the first layer to adding material to the second layer. This indicates that the first PFP monolayer largely completes before the second layer starts to nucleate. We observe this sharp cusp when growing PFP at substrate temperatures of 10 °C, 30 °C, and 70 °C demonstrating that within this temperature range the first monolayer mostly wets the substrate before 3d-growth sets in. The initial layer-by-layer growth breaks down during growth of the second monolayer, as can be seen from the fact that the anti-Bragg oscillation forms no second sharp cusp and the oscillation is damped out after growth of two monolayers. For a more quantitative understanding we analyzed real-time reflectivity measurements in a range from the total reflectivity edge to the first order Bragg reflection of PFP using the Parratt formalism [9]. With increasing deposition time (i.e. increasing deposited film thickness) the Bragg reflection increases and the Kiessig and Laue fringes get narrower (Fig. 3a). By successively fitting the reflectivity at fixed points in time [9] we extract the time dependent filling factors $\theta_n(t)$ of the individual layers as shown in Fig. 3b. The first layer nearly completes before significant second layer nucleation occurs, but the curves in Fig. 3b are smeared out due to the lower time resolution in wide q_z-range measurements and the fit uncertainties. Therefore the rather complete wetting of the first monolayer as inferred from the anti-Bragg oscillations is not perfectly reproduced. Third layer nucleation occurs early during deposition of the second layer, and the trend to early nucleation and 3d-growth increases for the following layers. From these layer filling factors $\theta_n(t)$ the standard deviation of the surface height from the nominal film thickness $\bar{d}(t)$ can be calculated according to

$$\sigma(t) = \sqrt{\sum_{n=0}^{\infty} (\theta_n(t) - \theta_{n+1}(t)) \cdot (15.7\text{Å} \cdot n - \bar{d}(t))^2} \qquad (1)$$

as a measure of the roughness σ (with $\theta_0(t) \equiv 1$ and $\theta_n(t) = 0$ for unfilled layers n) [7]. This evolution of the interface width σ is plotted in Fig. 3c and shows pronounced roughening already before completion of the second layer with σ increasing beyond the monolayer height of 15.7 Å. This behavior agrees with the results from the anti-Bragg measurement and is typical for Stranski–Krastanov growth where 3d-growth sets in after formation of a complete wetting layer. Compared to other organic semiconductors like PEN and diindenoperylene where layer-by-layer growth continues for up to four and seven monolayers respectively [8, 10] this early roughening is unfavorable for lateral charge transport [7]. This is partly offset though by the comparatively large in-plane size of the PFP islands and therefore lower grain boundary density, which leads to the attractive electron mobility of 0.049 cm^2 V^{-1} s^{-1} observed.

In conclusion, we have shown in this letter that thin films of the n-type semiconductor PFP deposited under suitable conditions (rate ~0.5 Å/min, substrate temperature 10–70 °C) on oxidized silicon wafers exhibit high crystalline order along the surface normal. The thin film crystal structure is close to the bulk phase and in contrast to PEN no contamination of the thin film with a second phase has been observed under the present conditions. Real-time measurements show that PFP grows in a Stranski–Krastanov growth mode with the first monolayer covering the substrate before 3d-growth sets in during growth of the second monolayer. Due to its high structural order PFP is an attractive n-type semiconducting material and the 3d-growth mode may be well suited for interdigitated p–n junctions e.g. in organic photovoltaic cells.

Acknowledgements We thank I. Salzmann and N. Koch for valuable comments, the EPSRC for financial support, and Kanto Denka Kogyo Co., Ltd. for providing the PFP.

References

[1] G. Horowitz, J. Mater. Res. **19**, 1946 (2004).
[2] Y. Sakamoto et al., Mol. Cryst. Liq. Cryst. **444**, 225 (2006).
[3] Y. Sakamoto et al., J. Am. Chem. Soc. **126**, 8138 (2004).
[4] A. Hinderhofer et al., J. Chem. Phys. **127**, 194705 (2007).
[5] N. Koch, et al., Adv. Mater. **19**, 112 (2007).
[6] Y. Inoue et al., Jpn. J. Appl. Phys. Part 1, **44**, 3663 (2005).
[7] F. Dinelli et al., Phys. Rev. Lett. **92**, 116802 (2004).
[8] S. Kowarik et al., Thin Solid Films **515**, 5606 (2007).
[9] O. Nelson, J. Appl. Crystallogr. **39**, 273 (2006).
[10] S. Kowarik et al., Phys. Rev. Lett. **96**, 125504 (2006).

